

Teleconnection between Seasonal Rainfall over East Africa and Global Sea Surface Temperature Anomalies

By **Laban J. Ogallo**

*Department of Meteorology
University of Nairobi, P.O. Box 30197, Nairobi, Kenya.*

and

J.E. Janowiak, M.S. Halpert

*Climate Analysis Centre
Washington D.C. 20233, U.S.A.*

(Manuscript received 3 February 1988, in revised form 6 July 1988)

Abstract

In this study, global sea surface temperature anomalies within $\pm 30^\circ$ latitudes of the equator were correlated with the time series of the major rotated principal component analysis (RPCA) modes of the seasonal rainfall over East Africa (Kenya, Uganda and Tanzania) for the period 1950-79. Regionally averaged rainfall anomalies were also correlated with the SST anomalies. The physical reality and climatological stability of the computed correlations were investigated using 6° by 6° gridmesh SST records instead of the original 2° by 2° values. The stability of the patterns were further tested by random removal of a maximum of upto five pairs of the SST and rainfall records from the original data sets. The results from the study indicate significant instantaneous (zero lag) and time lagged correlations between SST anomalies over portions of the global oceans and some of the principal seasonal rainfall modes in East Africa. The maximum instantaneous correlations occur in the boreal autumn between SST anomalies in the Pacific Ocean and the autumn rainfall RPCA mode, which is dominant over the coastal regions. The spatial patterns of the significant correlations indicate a 'see-saw' pattern between the eastern Pacific Ocean and the Indonesia region which coincides with positive rainfall anomalies over the coastal regions of East Africa, and indicates a relationship between rainfall variability in this region and the El Niño/Southern Oscillation (ENSO) phenomena. Lower spatial and temporal persistence is observed between SST anomalies and the rainfall RPCA modes that dominate inland. The maximum variance of the seasonal rainfall that could be accounted for by the SST anomalies was about 40%.

1. Introduction

The El Niño/Southern Oscillation (ENSO) phenomenon is known to be a fundamental and periodic part of the ocean-atmospheric system, with periodicity of seasonal to about 8 years

(Rasmusson and Carpenter, 1982). 'El Niño' or 'Warm episode' generally refers to anomalous warming of the eastern Pacific Ocean, while the term Southern Oscillation is used to describe the global zonal circulation centred around the 'sea-saw' pressure patterns between the western and eastern Pacific Ocean. ENSO signals have been

reported in many global parameters including pressure (Kidson, 1975), large scale convection (Egger *et al.* 1981, Wright 1984, Lau and Chan 1983), tropospheric temperatures (Horel and Wallace 1981), CO_2 concentration (Newell and Weare 1981), precipitation (Hastenrath and Heller 1977, Wright 1979, McBride and Nicholls 1983, Folland *et al.* 1986), Cyclone and Hurricane activities (Nicholls 1984), Monsoon circulations (Gadgil *et al.* 1984, Barnett 1984), oceanographic events (Cane 1982), as well as with non-meteorological parameters such as economic and biological consequences (Glantz 1984). Hastenrath and Heller (1977), among others have linked rainfall anomalies over the dry regions of north eastern Brazil to warm episode ENSO events. These events have also been associated with rainfall anomalies over Southern Africa (Hirst and Hastenrath 1983), New Zealand (Gordon 1986), Australia (McBride and Nicholls 1983), India (Parsatharathy and Pant 1985) and several tropical areas. Folland *et al.* (1986) associated the Sahel droughts to the enhanced warmth in the eastern south Pacific, south Atlantic and Indian Oceans, and cooler than normal conditions over the north Atlantic Ocean. Significant relationships among Sahel rainfall, the global sea surface temperatures (SST), and tropical circulation patterns have also been reported by Lamb (1978) and Lough (1986), among many others.

Over eastern, southern and equatorial Africa, extreme rainfall anomalies have also been linked to ENSO (Nicholson and Entekhabi (1986), Ogallo (1988a). Ogallo (1988a) observed significant teleconnections between the southern oscillation and seasonal rainfall over parts of East Africa, especially during the northern hemisphere autumn and summer seasons, with the strongest relationships being observed along the Kenyan coast during the autumn season. Recently, Janowiak (1988) showed evidence of an association between rainfall anomalies during austral summer over eastern and south eastern Africa and both the warm and cold phases of ENSO events.

In this study, an attempt will be made to further investigate teleconnections between East African seasonal rainfall, global SST anomalies, and the southern oscillation. The existence of

teleconnection between the SST anomalies and seasonal rainfall may prove very useful in the understanding of some of the physical factors which may be associated with the observed seasonal rainfall anomalies over the region.

The term East Africa will be used here to refer to three countries namely Kenya, Uganda and Tanzania. The region is located within latitudes 5°N - 12°S and longitudes 29°N - 43°S . East Africa has large spatial and temporal variations in rainfall due to the existence of complex topographical features, many large inland lakes and several other regional factors (Ogallo and Anyamba 1986).

Some examples of the seasonal rainfall patterns are given in figure 1 for some stations. The rainfall peaks centred around March-May and October-November months represent the two major rainfall periods for most parts of East Africa associated with the seasonal movements of the Inter Tropical Convergence Zone (ITCZ), which migrates seasonal with the other head Sun. The December-February rainfall peak (Fig. 1i) which is dominant over Southern Tanzania is also associated with the ITCZ characteristics in the southern hemisphere during the summer season.

Over the western parts of East Africa, especially most of Uganda and western Kenya, substantial rainfall is received throughout the year with another rainfall season centred around July/August (Fig. 1d-1h). This third rainfall season is associated with moisture influx from Atlantic ocean locally known as the 'Congo airmass'. The maximum influence of this westerly moisture incursions is during the northern hemisphere summer when the zonal and meridional components of the ITCZ are displaced furthest east and north respectively. Lake Victoria region, other western parts of Kenya together with the territory of Uganda which receive substantial rainfall throughout the year will be referred to in this text as the 'western regions'. A part from these 'western regions', substantial rainfall is also received near the other large water bodies which include the Indian Ocean, due to the influence of land/sea (lake) breeze. The diurnal and seasonal characteristics of these breezes over East Africa have been discussed by Asnani and Kinuthia (1979), Okeyo

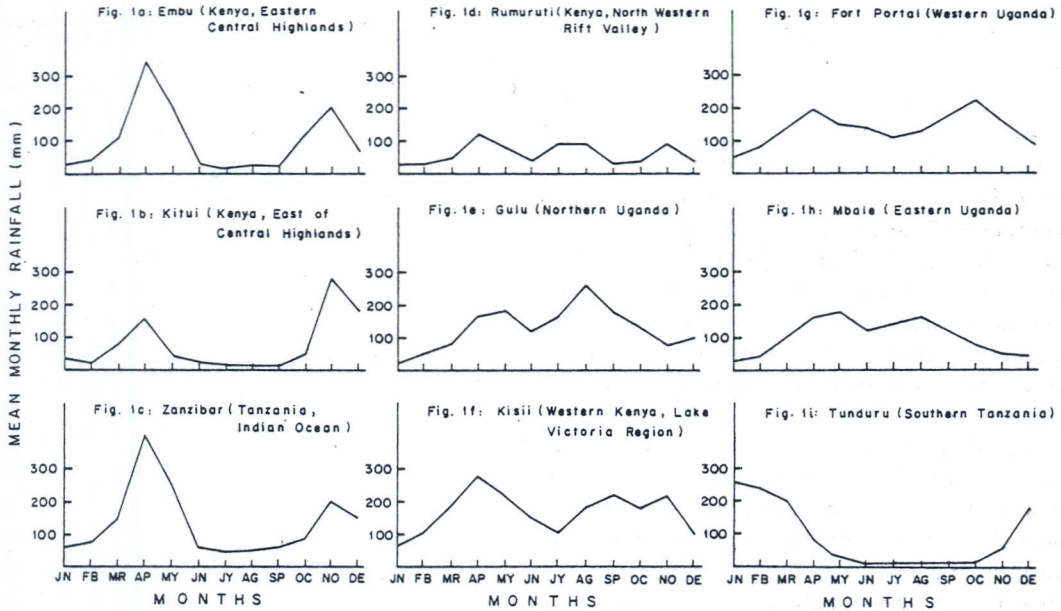


Fig. 1. Some examples of the East African seasonal rainfall patterns (locations are enclosed in the brackets).

(1986), among many others. Another factor which has been associated with the northern hemisphere summer rainfall along parts of the Indian Ocean coast is the East African low level jetstream which attains its peak intensity in July (Findlater 1977).

Although East Africa lies within the equatorial region where the synoptic scale winds are dominantly easterlies throughout the year at the low levels, the complex topographical patterns introduce significant modifications to the low level wind flow. These complex topographical features include the central highlands which run almost centrally across the region from north to south, together with the parallel rift valley. The central highlands restrict the moisture sources for most parts east of the highlands to the Indian ocean and Arabian sea, transported by the monsoonal wind systems. Many locations west of these highlands however, have the advantage of the Congo airmass and the existence of many large lakes like Victoria which is one of the largest fresh water lakes in the world. Lake Victoria and the mountain ranges induce semi-permanent troughs which persist throughout the year on the daily weather charts. Details of these

semi-permanent troughs, land/sea (lake) breezes together with the other physical features which have been associated with the time-space variability of rainfall over East Africa have been discussed by Ogallo and Anyamba (1986), Okeyo (1986), Asnani and Kinuthia (1979) among many others. These systems include the seasonal characteristics of the ITCZ, the Monsoon wind systems, tropical cyclones, four semi-permanent subtropical anticyclones, easterly waves, the African Jetstreams, global teleconnections, extratropical weather systems and thermally induced meso-scale circulations.

2. Data and methods

Under this section the various methods which were used to study the teleconnections between the East African seasonal rainfall and the global SST anomalies are highlighted. The data used in the teleconnection studies are however, presented first.

2.1 Sea surface temperatures and rainfall records

The sea surface temperature records were obtained from the Comprehensive Ocean Atmosphere Data Set (COADS) (Sultz *et al.*,

1985). Some problems associated with the COADS have been discussed by Jones *et al.* (1986), Land and Morrissey (1987) among others. These include the scarcity of data at some locations, the non-correction for the non-climatic effects and the duplication of the SST records at some locations. The data consist of global monthly SST anomalies on 2°N by 2° latitude/longitude squares, from 30°N to 30°S latitude, covering the period 1950-79. The monthly SST anomalies were computed by subtracting the long-term monthly means based on the 1950-79 period from the individual monthly means for each year.

The East African rainfall records used in this study consist of monthly records from about 91 stations (Fig. 2). The rainfall and SST records were then appropriately averaged to obtain seasonal records for the four standard meteorological season, relative to the northern hemisphere: summer (June-August), autumn (September-November) winter (December-February), and spring (March-May). In using a highly variable element like rainfall to study climatic fluctuations, areal averages are usually superior indicators of the regional climatic anomalies since they minimise the localised effects and other errors which may be associated with the individual measurements. Areal averaged records are also more representative of the general synoptic scale features.

Apart from using rainfall records from the individual rainfall stations, areal rainfall records derived from two methods were also independently used in the study. The first areal estimates of rainfall were obtained by subjecting the rainfall records for the individual seasons to rotated principal component analysis (RPCA). The inter seasonal characteristics of the dominant RPCA modes were then used to group East Africa into homogeneous rainfall regions. Details of the homogeneous rainfall groups may be obtained from Ogallo (1988a, b). Figure 3a however, gives the patterns of these regional categories. Areal rainfall estimates were computed for each of the 26 regions based on the arithmetic averages of all rainfall stations enclosed within the individual regions.

The major method which was used to derive

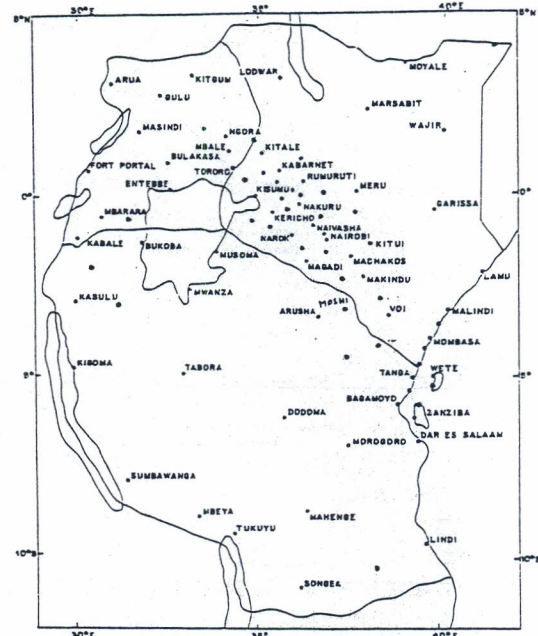


Fig. 2. Network of the rainfall stations used.

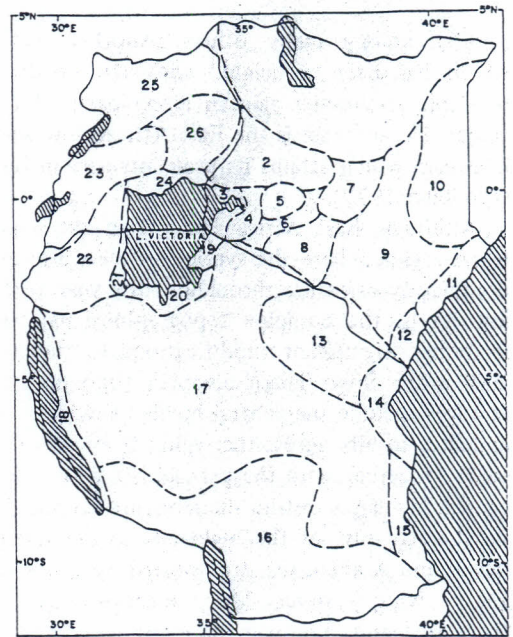


Fig. 3a. Homogeneous rainfall divisions derived from seasonal RPCA patterns (Ogallo 1988b).

areal rainfall indices was based on the time coefficients of the dominant rainfall RPCA modes. The use of time coefficients and other

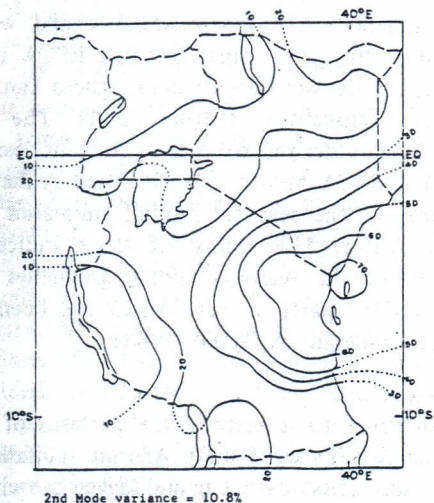


Fig. 3b. Mean patterns of the coastal rainfall RPCA mode (Northern Spring season).

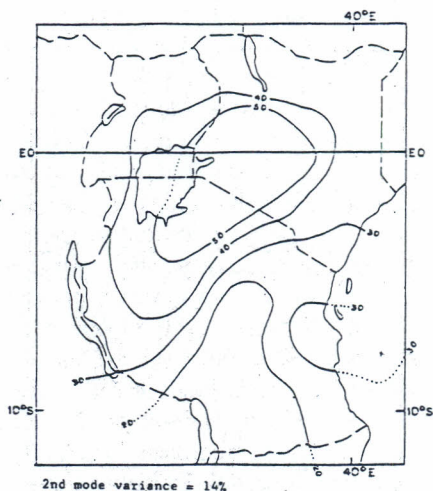


Fig. 3d. The spatial patterns of the migratory rainfall RPCA mode (N. Autumn season)

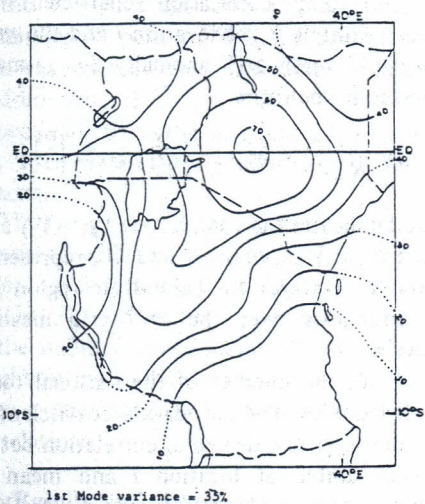


Fig. 3c. The spatial patterns of the migratory rainfall RPCA mode (N. Spring season).

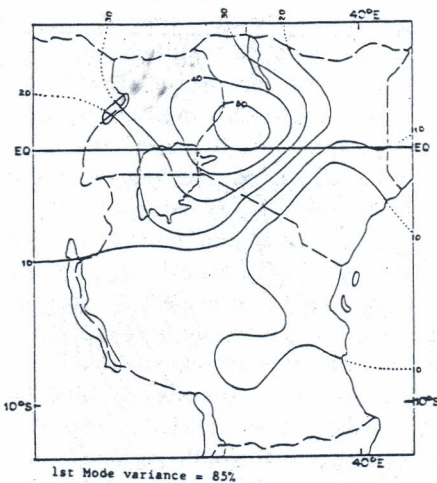


Fig. 3e. The spatial patterns of the migratory rainfall RPCA mode (N. summer season).

RPCA indices as areal estimates of highly varying climatic elements like rainfall has been discussed by Walsh and Mostek (1980), Johnson (1980), Richman (1981), Cohen (1983), Obled and Creutin (1986), and many others. The fundamentals of the time coefficients are therefore not discussed here.

Time-space variability of the dominant rainfall RPCA modes over East Africa have been discussed by Ogallo (1988a, b). The results from these studies indicated that although as many as seven eigenvectors were significant in some

months, especially during northern summer season, the patterns of the first three rainfall RPCA modes were outstanding throughout the year. Two of these RPCA modes dominated over the coastal and western regions respectively. The 'coastal region' here refer to the Indian Ocean coast where one of these RPCA modes dominated (Fig. 3b). In general the spatial patterns of the dominant RPCA mode shifted seasonally, closely resembling the ITCZ induced rainfall belts. The inter seasonal patterns of this RPCA mode are shown in figure 3c-3f. It is evident

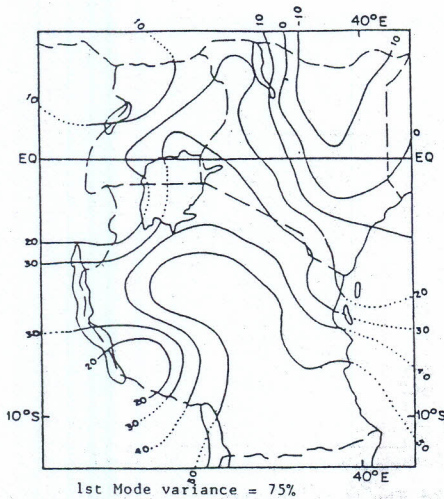


Fig. 3f. The spatial patterns of the migratory rainfall RPCA mode (N. Winter season).

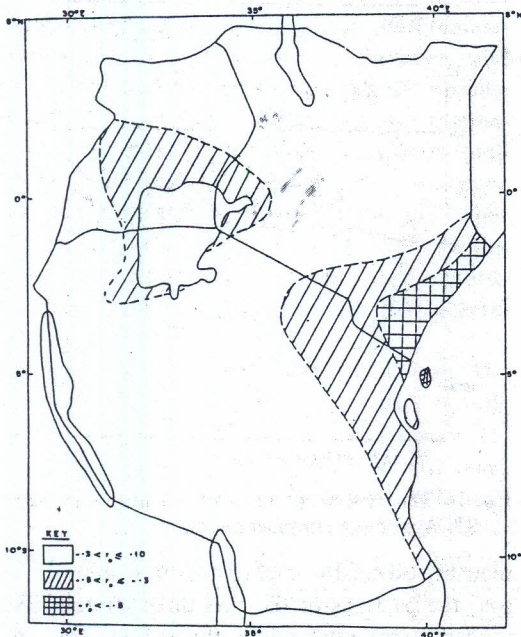


Fig. 3g. Zero lag correlation between SO and autumn coastal rainfall (Ogallo, 1988a).

from these patterns that during the spring and autumn seasons when most of East Africa is wet, this RPCA mode was dominant over most of the inland areas apart from southern Tanzania (Fig. 3c and 3d). The peak values were however, concentrated around equatorial Kenya. During

the northern hemisphere summer and winter seasons, the peak values for this RPCA mode shifted to the wet western and southern Tanzania regions respectively (Figure 3c-3f). The time coefficients derived from the dominant seasonal rainfall RPCA modes were also used as the area indices of the seasonal rainfall anomalies over East Africa. The ability of these indices in describing the seasonal rainfall anomalies over the various parts of East Africa has been discussed in details by Ogallo (1988a, b).

2.2 Methods

In order to investigate the patterns of teleconnection between East African rainfall and SST anomalies, Zero Lag and lagged correlation coefficients were computed for all pairs of seasonal rainfall and grid mesh SST anomalies. The Zero Lag correlation coefficient (r_{jm}) between rainfall X_{ij} at location j and the m^{th} 2° square grid mesh SST anomaly (Y_{im}) may be expressed in the form:

$$r_{jm} = \frac{1}{N} \left[\sum_{i=1}^N x_{ij} y_{im} \right] / \left[\sum_{i=1}^N x_{ij}^2 y_{im}^2 \right]^{1/2} \quad (1)$$

where i indicates the year, $x_{ij} = (X_{ij} - \bar{X}_j)$ and $y_{im} = (Y_{im} - \bar{Y}_m)$, while \bar{X}_j and \bar{Y}_m represent the arithmetic averages for rainfall at region j and SST anomalies over the m^{th} grid mesh respectively.

$N = 30$, the number of the seasonal records during 1950-79. The correlation coefficient r_{jm} therefore gives the degree of correlation between seasonal rainfall at location j and mean SST anomalies over the m^{th} square grid mesh.

The r_{jm} value for each grid mesh (m) and season was plotted at the centre of the grid mesh. The spatial patterns of the computed r_{jm} values were used to examine the patterns of teleconnections between East Africa seasonal rainfall records and the global SST anomalies within $\pm 30^\circ$ latitudinal bands. The statistical significance of the computed correlations were tested using t-test. Lagged correlation values were also computed for the various seasons by lagging the SST seasons and fixing the rainfall seasons. Significant time lag correlations between SST anomalies and seasonal rainfall can be of great use for the development of forecasting methods

for the seasonal rainfall anomalies.

3. The stability of the computed correlations

It is usually necessary to determine whether the patterns of the computed correlations are physically realistic and climatologically stable. These have been examined in this study by replacing the 2° square grid mesh SST anomalies with the corresponding 6° square values. The correlations between seasonal rainfall and the 6° square SST anomalies were again computed for all seasons. The stability of the correlation patterns were further investigated by subdividing the period of study into three subdivisions namely 1950-59, 1960-69, and 1970-79. One pair of the SST and rainfall records were then randomly removed from one of the subgroups, and correlation coefficients computed for each of the 2° square gridmesh SST values using the remaining 29 pairs of SST and rainfall records. This was repeated using data samples obtained by random removal of 2, 3, 4, and 5 pairs of records respectively from the subgroup. This procedure was then extended to other subdivisions and seasons.

The new correlation patterns were finally compared with the originally computed values in order to determine their spatial and temporal stability. The three decadal subperiods were used in the stability test to reduce the risk of choosing neighbouring rainfall records which could introduce some degree of persistence in the new correlations.

4. Results and discussion

The results obtained from the study will be discussed here basically under the two sections. The first part (4.1) will present the observed patterns of the zero lag correlations, while the final part (4.2) will be devoted to time lag correlations.

4.1 Zero lag correlations

The spatial patterns of the dominant rainfall RPCA modes indicated that there were significant differences in the temporal characteristics of rainfall over the coastal and inland regions (Ogallo 1988a, b), especially over the western, coastal and southern Tanzanian regions. The

teleconnection patterns with the inland and coastal regions are therefore highlighted independently under this section.

Figure 4 gives the spatial patterns of the Zero lag correlation between 2° square gridmesh SST anomalies and the amplitude time series of the various RPCA modes which were dominant over the coastal region of the Indian ocean during the same season. The figure indicates that maximum correlations were observed during the boreal Autumn season (Fig. 4a). Autumn is generally the second (short) rainy season over many parts of East Africa, associated with the second passage of the Inter-Tropical Convergence Zone (ITCZ). The maximum positive correlations which were observed during the autumn season, are concentrated over the equatorial central and eastern Pacific Ocean.

Large negative values of the Zero lag correlation were, however, observed over the western Pacific ocean and most of Indonesia. Peak values of these correlations are near 0.60.

'See-saw' patterns (adjacent regions of strong positive and negative correlation) have been observed in many general circulation parameters that are associated with fluctuations in the Walker Circulation and with the inter-related ENSO episodes (Walker (1923), Berlage (1966), Troup (1965), Trenberth (1976), Wright (1985), Rasmusson and Carpenter (1982)). An example of this dipole characteristic is shown in Figure 5 which illustrates the spatial pattern of the global barometric correlation with Djakarta sea level pressure (Berlage, 1966). It is apparent from this figure that the maximum barometric correlations over the African continent are concentrated within the equatorial East African coast. The inverse nature of the barometric and SST correlation patterns are quite evident in Figure 4a and 5. The strongest relationship between East Africa seasonal rainfall and the Southern oscillation has been observed along the coastal region as well, during the northern autumn season (Fig. 3g, Ogallo, 1988a). Figure 4a further indicates that the boreal autumn rainfall anomalies over the coastal regions of East Africa are positively correlated with SST anomalies over the Arabian Sea, equatorial eastern, central and northern Indian Ocean. Low correlations are observed over

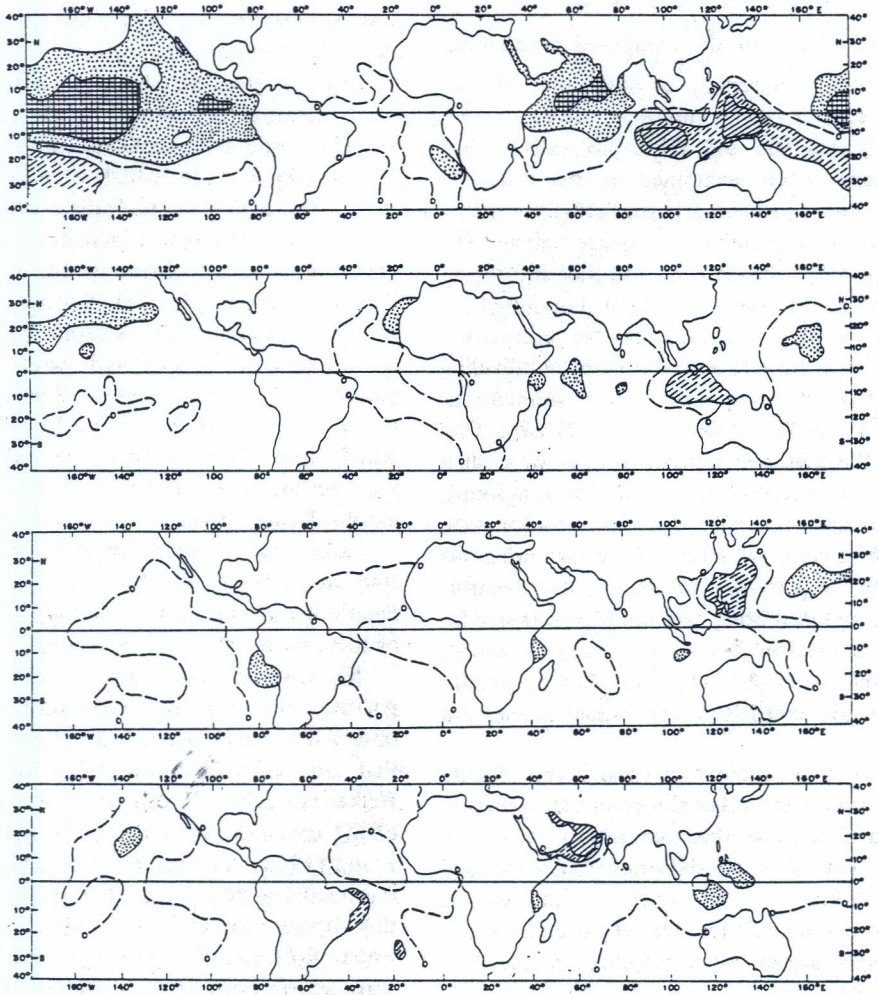


Fig. 4. Instantaneous correlations between SST anomalies and the rainfall RPCA modes dominant over the coastal region during (a) Autumn (b) Summer (c) Spring (d) Winter seasons.

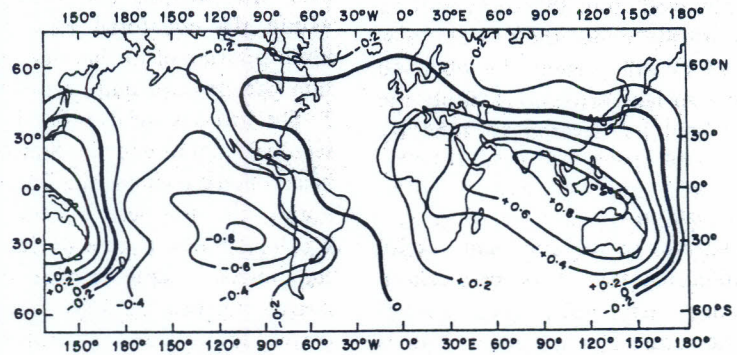


Fig. 5. Global patterns of the correlation between sea level pressure at Jakarta and other locations throughout the world (Berlage 1966).

most of the Atlantic Ocean, apart from some isolated parts of the southwest coast of southern Africa.

Positive SST anomalies, especially over the equatorial eastern and northern Indian Ocean and the Arabian Sea regions, may be associated with the weakening of the north easterly monsoonal winds and the strengthening of the south easterlies from the southern Indian Ocean. Such characteristics have been associated with some wet episodes over parts of Eastern Africa (Cade and Diehl (1984), Cadet (1985), Ogallo and Anyamba (1986). Other major physical features of some of the positively correlated regions of the Indian Ocean include upwelling, the strong Somalia Ocean currents, and the East African low level jet (Findlater (1986), Scott (1983)). The spatial patterns of the correlations between SST anomalies and the rainfall RPCA modes that indicate dominance over the coastal regions during the northern summer, spring, and winter seasons are given in Figures 4b-d, respectively. It can be observed from Figures 4b and 4c that the 'see-saw' correlation patterns which are observed over the Pacific Ocean region during the autumn season are also evident during the northern summer and spring seasons, although the areal extent and magnitude of the correlations are smaller especially during the spring season.

Figure 4d indicates that the spatial patterns of the Zero lag correlations during the winter season are significantly different from those observed during the previous seasons. During winter rainfall over the coastal areas of East Africa appears to be negatively correlated with SST anomalies over the Arabian Sea region, where correlation values in the range of -0.5 are observed. Since the ITCZ is located over southern Africa during the winter season the moisture sources for coastal East Africa are predominantly from the Arabian Sea region and the north eastern Indian Ocean. Negative SST anomalies over the Arabian Sea region would therefore favour the strengthening of the maritime components of the north easterly monsoon winds, and hence favour increased rainfall in coastal East Africa. And since positive SST anomalies tend to be observed over coastal East Africa during this situation (Fig. 4d), it is reasonable to conclude that more intense

convection is also implied in this region. Significant positive correlations in northern winter between SST anomalies are also observed. Coastal East Africa is generally wet throughout the year, although the moisture sources vary seasonally, depending on the dominant component of the monsoonal winds. Some of these wind components are more laden with moisture. The impacts of these wind systems and other associations with rainfall have been discussed by Cade *et al.* (1985), Barnett (1984), Ogallo and Anyamba (1986). The high degree of spatial and temporal persistence in the SST anomalies are also reflected in the results of the study. Similar patterns of seasonal persistence were also observed between East Africa seasonal rainfall and SO (Ogallo 1988a). Relationships between rainfall and SST anomalies are further demonstrated in Figure 6a and 6b. Figure 6b gives the time coefficients of the first SST RPCA mode for the Pacific Ocean during the northern autumn season. The spatial patterns of this SST RPCA mode are shown in figure 6c. It is evident from figures 6a and b that significant associations existed between some of the extreme SST and rainfall anomalies.

The instantaneous correlations between the SST anomalies and the rainfall RPCA modes that are dominant over the western portions of the inland areas are shown in Figure 7, for each season. Most of the inland areas are wet during the boreal Autumn and Spring seasons, corresponding to each passage of the ITCZ. The western portion of this region where rainfall is highly influenced by the westerly moisture influx from Atlantic Ocean and the moist Zaire/Congo regions together with the existence of the large inland lakes, have rainfall throughout the year. It can be observed from Figure 7 that although significant instantaneous correlation are observed between SST anomalies and the composite rainfall indices for the western inland parts especially during the northern summer and autumn seasons, the magnitudes of the spatial and temporal persistence are relatively low compared to those observed with the composite rainfall indices for the coastal region during the autumn season. Figure 7 also indicates that the maximum instantaneous correlations are observed between

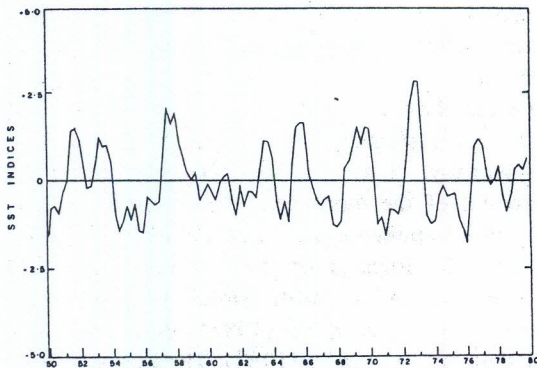


Fig. 6a. Time series of the first Autumn SST RPCA mode over the Pacific Ocean for 6° by 6° grid mesh values.

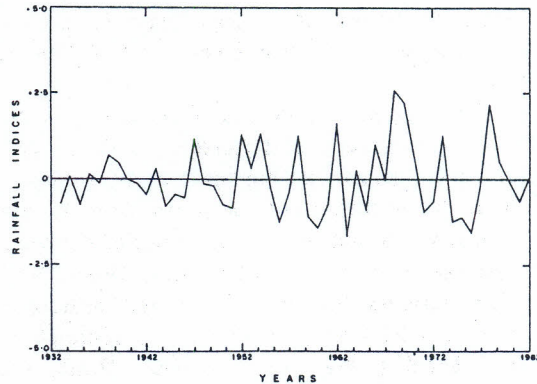


Fig. 6b. Time series of the rainfall RPCA mode dominant over the coastal region.

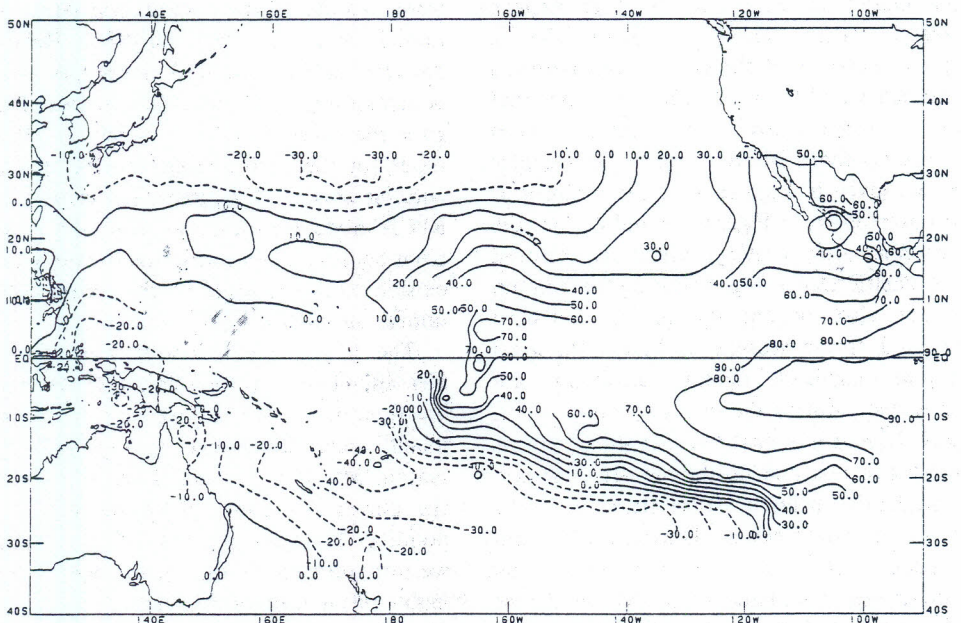


Fig. 6c. The spatial patterns of the first RPCA mode over the Pacific Ocean.

the rainfall RPCA modes that are dominant over the western regions and SST anomalies during the northern summer season.

It is apparent that the correlation patterns between rainfall and SST anomalies during autumn for coastal region (Fig. 4a) and for the western portions of inland East Africa during summer (Fig. 7a) are quite opposite in nature. The feature is most evident over the central and eastern Pacific Ocean. Similar but relatively lower degree of persistence were also observed

during the northern winter season (Figure 7d).

The negative correlation values observed over the central and eastern Pacific during the summer (Fig. 7a) indicate that negative summer rainfall anomalies over the western regions have a tendency to occur during ENSO warm episodes. Similar characteristics have been observed, especially during summer, by Ogallo (1988a) who used a Southern Oscillation index derived from the normalized difference of monthly Tahiti and Darwin sea level pressure (Tahiti

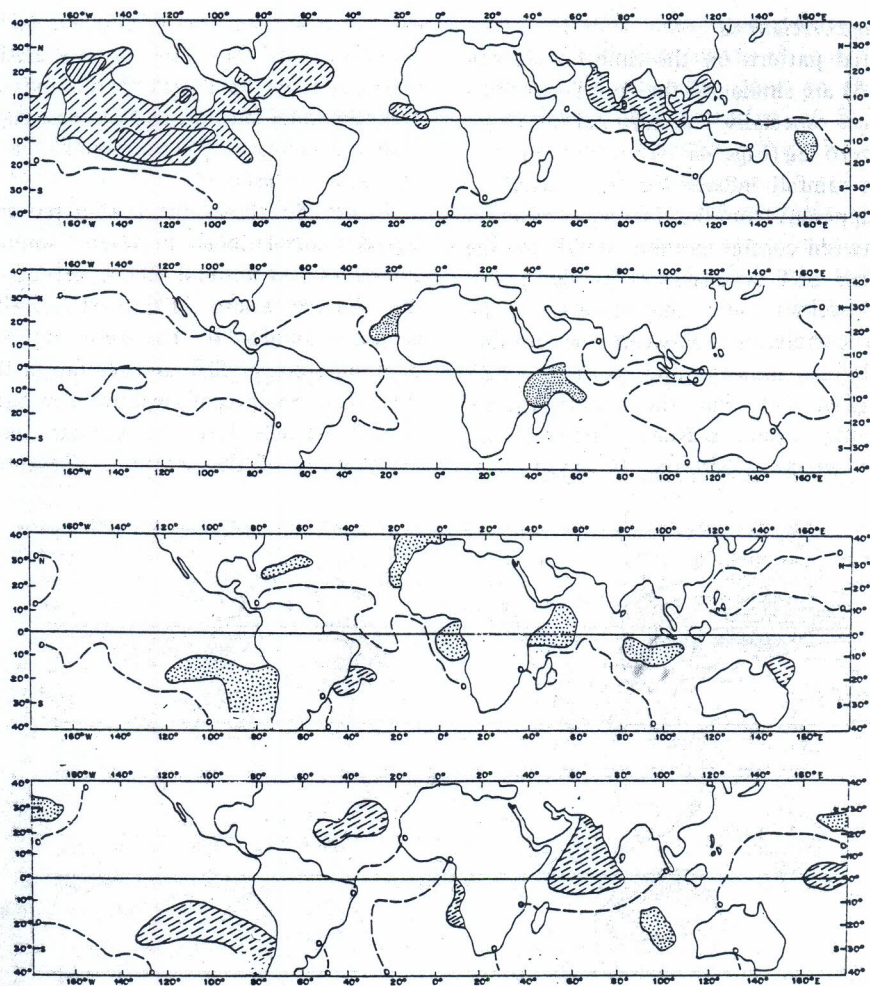


Fig. 7. Zero lag correlations between SST anomalies and the rainfall modes dominant western regions during (a) Summer (b) Autumn (c) Spring (d) Winter seasons.

minus Darwin) as a measure of the state of the Southern Oscillation. Figure 7a also indicates significant negative correlations among the summer rainfall over the western regions and SST anomalies over parts of the equatorial Atlantic Ocean, north eastern Indian Ocean, and the Arabia Sea region. Negative SST anomalies, with the resultant intensification of sea level pressure over these anomalous regions, favours the influx of moist air into East Africa.

The positive correlation between western region and SST anomalies in the equatorial Atlantic in northern spring (Fig. 7c), and the

western Indian Ocean region during northern autumn and spring (Fig. 7b, c) may be the reflection of the relaxation of the surface pressures over the equatorial regions due to the passage of ITCZ.

Positive SST anomalies over coastal north western Africa (within the region of influence of the Azores anticyclone) would also tend to reduce the influx of the modified dry sahelian air mass into western regions due to the relaxation of the sea level pressures.

4.2 Time lag correlations

The spatial pattern on the time lag correlations (Fig. 8) are similar to the zero lag correlation patterns, especially the seasonal lag (Figs. 8a, b) and zero lag (Figs. 4a, b) correlations with the autumn rainfall indices for the coastal regions. It is apparent from the time lag correlation patterns between coastal autumn rainfall and the spring/summer SST anomalies (Figs. 8a, b, respectively) together with the patterns of instantaneous correlations between the autumn coastal rainfall indices and autumn SST anomalies (Fig. 4a) that these patterns are persistent over several seasons. The zero lag correlation 'see-saw' patterns observed over

eastern and western Pacific Ocean are also discernible in the time lag correlations. The magnitude of the lagged correlations are, however, generally smaller, and decrease significantly with the increase in the seasonal time lags from the autumn season.

Figure 8c shows the spatial pattern of the lagged correlations between summer SST anomalies and autumn RPCA rainfall mode for the 'western regions' of East Africa. The pattern is quite similar to the zero lag correlation between summer SST and rainfall in this region (Fig. 7a). Significant negative correlation with rainfall persists into the autumn season over many parts of the central and eastern Pacific

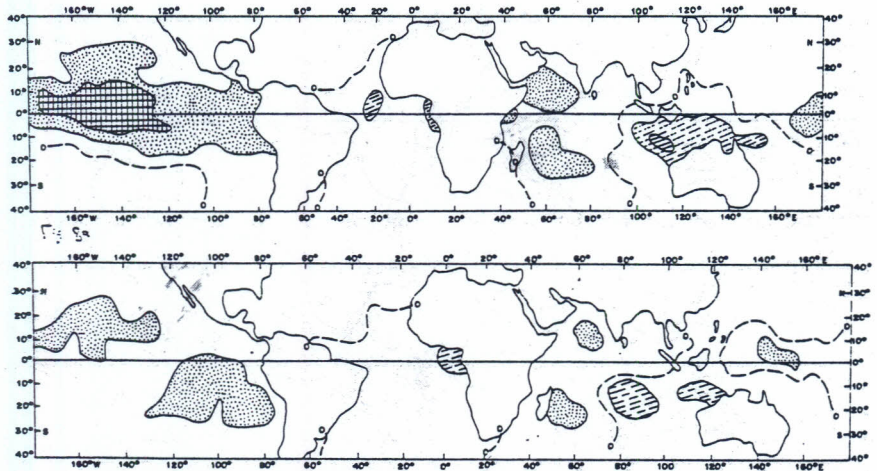


Fig. 8. Lag correlations between Autumn coastal rainfall indices and (a) Summer (b) Spring SST anomalies.

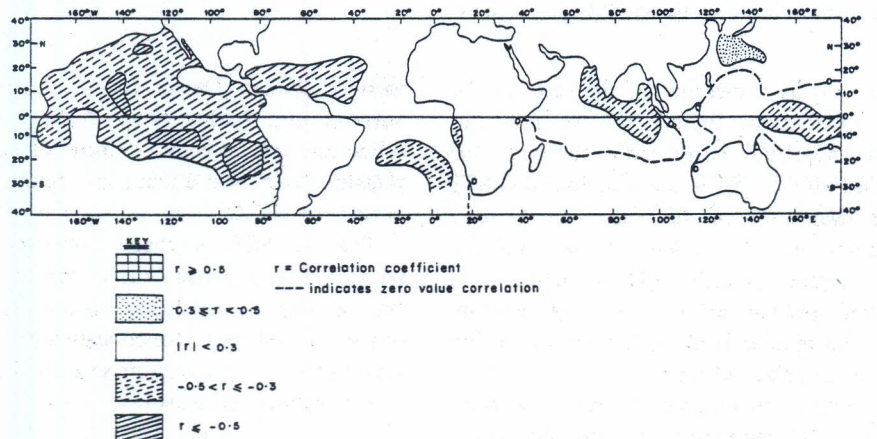


Fig. 8c. Lag correlations between summer SST anomalies and Autumn rainfall indices for the western regions.

Ocean. The similarities in the patterns of the zero lag and lagged correlations reflects the persistent nature of the SST anomalies.

The physical reality and the climatological stability of the instantaneous and the time lag correlation as depicted from the 6° square grid mesh SST analyses are shown in figure 9 for the autumn and summer seasons. High degree of similarities with the correlations of the 2° square SST anomalies are evident from Figures 4, 7 and 8. Patches of correlations which were observed

over Atlantic ocean were however, not discernible with most of the 6° square SST records. This could be partly due to the large area included in the averaging of SST anomalies. Similar characteristics were also evident over some parts of global oceans.

Relatively identical patterns were also obtained by the random omission of a maximum of upto five pairs of SST and rainfall records, reflecting significant spatial and temporal stability of the observed correlation patterns.

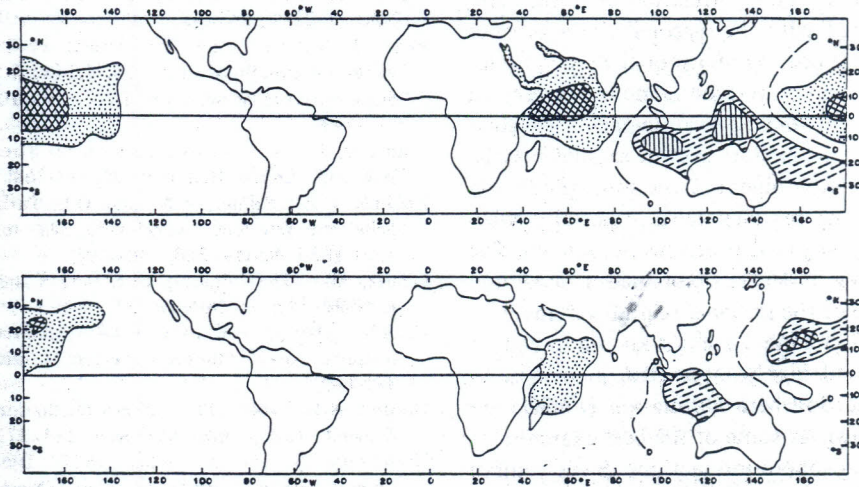


Fig. 9. (a) Autumn (b) Summer zero lag correlations between 6° by 6° grid mesh SST anomalies, and the coastal rainfall indices.

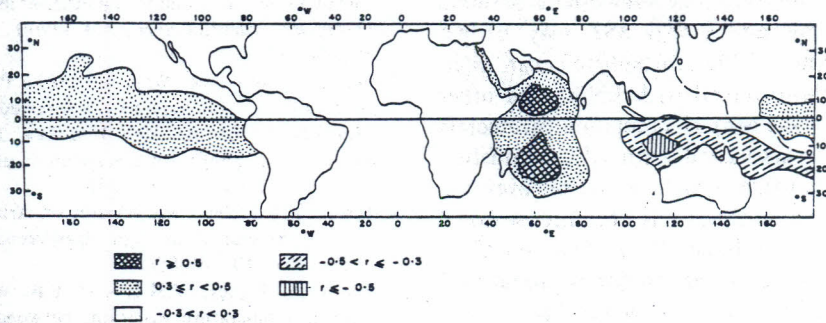


Fig. 9b. Lag correlation between autumn rainfall anomalies over region twelve (Figure 3a) and the 6° by 6° grid mesh SST anomalies.

5. Conclusions

Results from this study indicate significant instantaneous and time lag correlations between SST anomalies over parts of the global oceans and some seasonal rainfall modes over parts of East Africa, especially during the boreal summer

and autumn seasons. The maximum instantaneous and lagged correlation values are observed between SST anomalies over the Pacific Ocean and the autumn rainfall RPCA mode which is dominant over coastal East Africa. 'See-saw' correlations patterns in both the zero

lag and seasonally lagged correlation between SST and rainfall anomalies are apparent over the western and eastern Pacific Ocean. Significant correlations are also observed over portions of the Indian Ocean throughout the year, especially near the coastal of East Africa and Somalia, the North-eastern Indian Ocean and the Arabian Sea. Inland from the coast, the maximum correlation was observed between SST anomalies over the western Pacific and the summer rainfall modes which were dominant over the western regions of the East Africa. The correlation patterns have been associated with the seasonal characteristics of the moisture-bearing monsoonal wind systems. The significant teleconnections observed between rainfall and SST anomalies over parts of the global oceans during some seasons may be useful in the development of the some prediction methods for the seasonal rains, especially when all underlying physical processes are known. The SST anomalies, however, explained a maximum of about 40% of the seasonal rainfall variance.

The global climate system is known to consist of complex and highly interactive processes. El Niño and the Southern Oscillation (ENSO) are however, known as some of the best examples of the ocean-atmosphere interactions. Since rainfall anomalies over parts of the Eastern Africa have been associated with ENSO, the physical basis of some of the observed teleconnections between seasonal rainfall and global SST may be explained in terms of the atmosphere-ocean interactions like those linked with ENSO and other components of the general circulation parameters which may be associated with SST anomalies. Another phenomena which is active over the Pacific and Indian Oceans is the inter-seasonal wave (Madden and Julian 1971, Lau and Chan 1983). The physics of Eastern Africa rainfall and SST correlations have however not been thoroughly investigated, and are currently forming the basis of many regional studies.

References

- Asnani, G.C. and J.H. Kinuthia, 1979: Diurnal variation of precipitation in East Africa. *E. Africa Met. Dept. Memo.* 8, 58pp.
- Barnett, T.P., 1984: Interactions of the monsoon and Pacific Trade wind system at inter annual time scales. Part III: A Partial Anatomy of the Southern Oscillation. *Mon. Wea. Rev.*, **112**, 2389-2400.
- Berlage, H.P., 1966: Fluctuations in the general circulation of more than one year, their nature and prognostic value. *KNMI Meded Vern.* **69**.
- Cadet, D.L. (1985): The Southern Oscillation over Indian Ocean. *J. Climatol.*, **5**, 189-212.
- Cadet, D.L., and B. Diehl, 1984: Inter annual variability of the surface field over the Indian Ocean during the recent decades. *Mon. Wea. Rev.*, **112**, 21-25.
- Cohen, S.T., 1983: Classification of 500mb height analysis using obliquely rotated Principal Components. *J. Climate Appl. Met.*, **220**, 1975-88.
- Cane, M.H. 1982: Oceanographic events during El Niño. *Science*, **22**, 1189-1195.
- Egger, J., Meyers, G. and P.B. Wright, 1981: Pressure, wind and cloudiness in the tropical Pacific related to Southern Oscillation. *Mon. Wea. Rev.*, **109**, 1139-1149.
- Findlater, J., 1977: Cross-equatorial Jet Stream at low level over Kenya. *Kenya. Met. Mag.*, **95**, 353-364.
- Folland, C.K., Palmer, T.N. and D.E. Parker, 1986: Sahel rainfall and world-wide sea temperature 1901-1985. *Nature*, **320**, 602-609.
- Glantz, M., 1984: Floods, Fires and Famines. It is El-Niño to blame. *Oceanus*, **27**, 14-19.
- Gadgil, S., Joseph, P.V. Joshi, 1984: Ocean-Atmosphere coupling over monsoon regions. *Nature*, **312**, 141-143.
- Gordon, N.D. 1986: The Southern Oscillation and New Zealand weather. *Mon. Wea. Rev.*, **114**, 371-396.
- Hastenrath, S. and L. Heller, 1977: Dynamics of Climatic hazards in N.E. Brazil. *Quart. J. Roy. Meteor. Soc.*, **103**, 77-93.
- Hist, A.C. and S. Hastenrath, 1983: Atmosphere-ocean mechanisms of climate anomalies in the Angola Tropical Atlantic Sector. *J. Phys. Ocean.*, **13**, 1143-1157.
- Horel, J.D. and J.M. Wallace, 1981: Planetary-scale atmospheric phenomena associated with the Southern Oscillation. *Mon. Wea. Rev.*, **109**, 813-829.
- Janowiak, J.E., 1988: An investigation of inter-annual rainfall. *J. Climate*, **1**, 240-255.
- Johnson, D.N. 1980: An Aindex of Arizona summer rainfall developed through eigen-vector analysis. *J. Appl. Met.*, **19**, 849-856.
- Jones, P.D., Wigley, T.M.L. and P.B. Wright, 1986: Global temperature variations between 1861-1984: *Nature*, **322**, 430-434.
- Kidson, J.W., 1975: Tropical eigen-vector analysis and Southern Oscillation. *Mon. Wea. Rev.*, **103**, 187-196.
- Lau, K. and P.H. Chan, 1983: Short term climate Variability and Atmospheric Teleconnections from Satellite observed Outgoing Longwave Radiation. Part I Simulation Relationships. *J. Atmos. Soc.*, **40**, 2735-2750.
- Lamb, P.J., 1978: Large Scale Tropical Atlantic surface circulation patterns associated with Sub Saharan

weather anomalies. *Tellus*, **30**, 240-251.

- Lander, M.A. and M.I. Morrissey, 1987: Unexpected Duplicate ship reports in the COADS. *TOGA Newsletters*, March, 1987, 13-14.
- Lough, J.M., 1986: Tropical sea surface temperatures and rainfall variation in sub-sahara Africa. *Mon. Wea. Rev.*, **114**, 561-570.
- Madden, R.A. and P.R. Julian, 1971: Detection of a 40-50 day oscillation in the zonal wind in the tropical Pacific Ocean. *J. Atmos. Sci.*, **28**, 702-708.
- McBride, J.L. and N. Nicholla, 1983: Seasonal relationships between Australian rainfall and Southern Oscillation. *Mon. Wea. Rev.*, **111**, 1998-2004.
- Newell, R.E. and B.Sc. Weare, 1976: Factors governing troposphere mean temperatures. *Science*, **194**, 1413-1414.
- Nicholls, N. 1984: The Southern Oscillation, Sea-surface Temperature and inter annual fluctuations in Australian Tropical Cyclone activity. *J. Climatol.*, **4**, 661-670.
- Nicholson, S.E. and D. Etekhabi, 1986: The quasi-periodic behaviour of rainfall variability in Africa and its relationship to the Southern Oscillation. *Arch. Met. Geophys. Bioh. Ser.*, **A34**, 322-348.
- Okeyo, A.E., 1986: The influence of Lake Victoria a convective systems over the Kenyan Highlands Proc. *International Conference on short medium range forecasting*, August, 1986, Tokyo, Japan.
- Obled, C. and J.D. Creutin, 1986: Some developments in the use of empirical orthogonal functions for mapping meteorological fields. *J. Appl. Met.*, **25**, 1189-1204.
- Ogallo, L.J., 1988: Relationships between seasonal rainfall in East Africa and the Southern Oscillation. *J. Climatol.*, **8**, 31-43.
- Ogallo, L.J., 1988b: The spatial and temporal clusters of the East Africa seasonal rainfall anomalies derived from Principal component Analysis, *J. Climatol.*, **8**, 1-23.
- Ogallo, L.J. and E.K. Anyamba, 1986: Droughts of the tropical Central and Eastern Africa, July-November, 1983. Northern Spring (1983-84). *Reprints from 1st WMO Workshop on Diagnosis and prediction of Monthly and seasonal variations over the Globe College Park, U.S.A. WMP/TD*. No. 87, 67-72.
- Parasatharathy, B. and G.B. Pant, 1985: Seasonal relationship between Indian summer monsoon rainfall and the Southern Oscillation. *J. Climatol.*, **5**, 369-378.
- Rasmusson, E.M. and R.D. Carpenter, 1982: Variation in the tropical seas surface temperatures and sea wind fields associated with the southern oscillation/El Nino. *Mon. Wea. Rev.*, **110**, 354-384.
- Richman, M.D., 1981: Obliquely rotated principal components. An improved meteorological map typing technique. *J. Appl. Met.*, **20**, 1145-1159.
- Scott, J. 1983: Monsoon response of the Somalia current and associated upwelling. *Prog. Ocean*, **12**, 357-381.
- Slutz, R.J. et al. 1985: Comprehensive Ocean-Atmosphere Data Set. *NOAA Environment Research Laboratories Boulder, U.S.A.*
- Trenberth, K.E., 1976: Spatial and temporal variations of the Southern Oscillation. *Quart. J.R. Met. Soc.*, **102**, 639-653.
- Troup, A.J., 1965: The Southern Oscillation. *Ibid.*, **91**, 490-506.
- Walsh, J.E. and A. Mostek, 1980: A quantitative analysis of meteorological anomaly patterns over United States, 1900-1971. *Mon. Wea. Rev.*, **108**, 615-630.
- Wright, P.B. 1979: Persistence of rainfall anomalies in the Central Pacific, *Nature*, **277**, 371-374.
- Wright, P.B., 1984: The possible role of cloudiness in the Southern Oscillation. *Nature*, **310**, 128-130.
- Wright, P.B., 1985: The Southern Oscillation: An Ocean-Atmosphere Feedback System. *Bull. Amer. Meteor. Soc.*, **66**, 398-412.

東アフリカにおける季節的降水量と全球海面水温とのあいだのテレコネクション

Laban L. Ogallo

(ナイロビ大学 気象学科)

J. E. Janowiak and M. S. Halpert

(NOAA 気候解折センター)

この研究では、 30° より低緯度側の全球海面水温 (SST) と、東アフリカ (ケニア、ウガンダ、タンザニア) の季節的降水量の回転主成分分析 (RPCA) の主なモードとの相関を、(1950-79)の期間について調べた。地球ごとに平均された降水量と SST との相関も調べた。計算された相関の物理的現実性と気候学的安定性も、もとの $2^\circ \times 2^\circ$ グリッドの SST データのかわりに、 $6^\circ \times 6^\circ$ SST データを用いることにより調査した。パターン安定性はさらに、SST と降水量のもとの時グリッドの系列データセットから最大 5 組のランダムな記録を取り除くことによって、検定された。その結果、全球的な海洋のいくつかの地域と東アフリカの季節的降水量のいくつかの主なモードとのあいだに、有意な同時及び時差の相関のあることがわかった。最大の同時期間は北半球秋における太平洋での SST と、海岸地域に卓越する秋雨との間のシーズンパターンを示しこれは東アフリカ海岸地域で RPCA モードとの間に見出された。この有意な相関の空間パターンは東太平洋とインドネシア地域での降水量の正偏差と一致してあらわれており、この地域の降水量変動が ENSO 現象と関係していることを示している。SST と内陸域に卓越する RPCA との相関は、空間的にも時間的にもより低い持続性を示している。SST 偏差で説明できる季節的降水量の極大の分散は約 4% である。